Title

Tunneling nanotubes mediate the expression of senescence markers in mesenchymal stem/stromal cell spheroids

Journal

Stem Cells, 38(1)

ISSN

1066-5099

Authors

Whitehead, Jacklyn
Zhang, Jiali
Harvestine, Jenna N
et al.

Publication Date

2020

DOI

10.1002/stem.3056

Peer reviewed

HHS Public Access

Author manuscript

Stem Cells. Author manuscript; available in PMC 2021 January 01.

Published in final edited form as:

Stem Cells. 2020 January ; 38(1): 80–89. doi:10.1002/stem.3056.

Tunneling Nanotubes Mediate the Expression of Senescence Markers in Mesenchymal Stem/Stromal Cell Spheroids

Jacklyn Whitehead[1,†], **Jiali Zhang**[2,†], **Jenna N. Harvestine**[1], **Alefia Kothambawala**[1], **Gang-yu Liu**[2,*], **J. Kent Leach**[1,3,*]

[1]Department of Biomedical Engineering, University of California, Davis, CA 95616

[2]Department of Chemistry, University of California, Davis, CA 95616

[3]Department of Orthopaedic Surgery, UC Davis Health, Sacramento, CA 95817

Abstract

The therapeutic potential of mesenchymal stem/stromal cells (MSCs) is limited by acquired senescence following prolonged culture expansion and high passage numbers. However, the degree of cell senescence is dynamic, and cell-cell communication is critical to promote cell survival. MSC spheroids exhibit improved viability compared to monodispersed cells, and actin-rich tunneling nanotubes (TNTs) may mediate cell survival and other functions through the exchange of cytoplasmic components. Building upon our previous demonstration of TNTs bridging MSCs within these cell aggregates, we hypothesized that TNTs would influence the expression of senescence markers in MSC spheroids. We confirmed the existence of functional TNTs in MSC spheroids formed from low passage, high passage, and mixtures of low and high passage cells using scanning electron microscopy, confocal microscopy, and flow cytometry. The contribution of TNTs toward the expression of senescence markers was investigated by blocking TNT formation with cytochalasin D (CytoD), an inhibitor of actin polymerization. CytoD-treated spheroids exhibited decreases in cytosol transfer. Compared to spheroids formed solely of high passage MSCs, the addition of low passage MSCs reduced *p16* expression, a known genetic marker of senescence. We observed a significant increase in *p16* expression in high passage cells when TNT formation was inhibited, establishing the importance of TNTs in MSC spheroids. These data confirm the restorative role of TNTs within MSC spheroids formed with low and high passage cells and represent an exciting approach to utilize higher passage cells in cell-based therapies.

Graphical Abstract

[*]**authors to whom correspondence should be addressed** J. Kent Leach, Ph.D., University of California, Davis, Department of Biomedical Engineering, 451 Health Sciences Drive, 2303 GBSF, Davis, CA 95616, jkleach@ucdavis.edu, Gang-yu Liu, Ph.D., University of California, Davis, Department of Chemistry, One Shields Avenue, 322 Chemistry, Davis, CA 95616, gyliu@ucdavis.edu.

[†]Authors contributed equally

DISCLOSURE OF CONFLICTS OF INTERESTS

All of the authors have declared no conflict of interest.

DATA AVAILABILITY STATEMENT

The data that support the findings of this study are available from the corresponding author upon reasonable request.

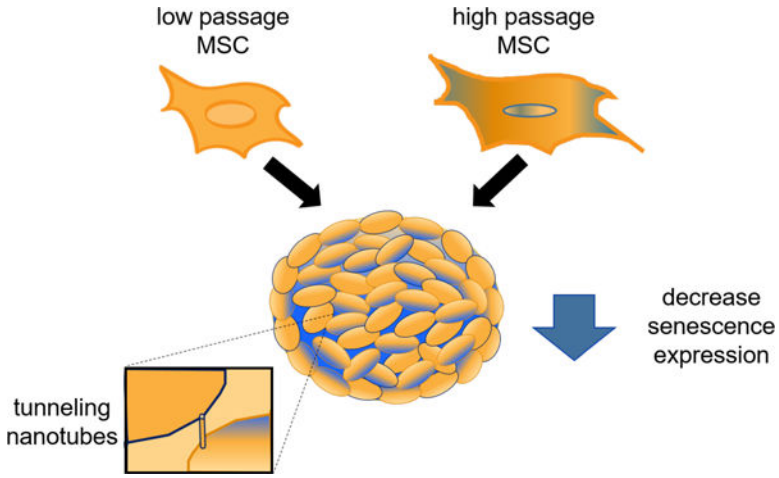

Keywords

Tunneling nanotubes; mesenchymal stem/stromal cells; senescence; spheroids; *p16*

INTRODUCTION

Mesenchymal stem/stromal cells (MSCs) hold widespread appeal for use in tissue engineering due to their ease of acquisition, multilineage potential, and potent secretome that provides proangiogenic and anti-inflammatory cues to promote tissue repair.[1,2] The limited number of MSCs that can be retrieved from tissue aspirates necessitates prolonged culture expansion to achieve clinically relevant numbers. Extensive passaging of MSCs can induce replicative senescence, resulting in cell cycle arrest, impaired function, or loss of the regenerative phenotype.[3]

Senescence, the state of arrested cell growth without apoptosis, is characterized by an enlarged flat cellular morphology, expression of senescence-associated β-galactosidase (SAβ-gal) activity, DNA damage, enhanced expression of regulatory proteins, and the senescence-associated secretory phenotype (SASP).[4] Senescence is a multi-step, progressive process that is distinct from the more reversible quiescent state.[5] Senescence has been widely regarded as an irreversible mechanism that models aging, but recent discoveries indicate that senescence is not a static endpoint nor wholly detrimental to an organism.[6] In fact, several studies report that the physiological relevance of senescence extends beyond suppression of tumorigenesis and modeling organismal aging into biological processes such as embryonic development[7], wound healing[8], and tissue repair.[9]

Cells reside in a three-dimensional environment that is rich in extracellular proteins and cell-cell contact, yet senescence is commonly studied in monolayer culture. In contrast to monolayer culture, MSCs aggregated into spheroids retain a supportive extracellular matrix (ECM) and engage in cell-cell contact that better recapitulates a native tissue environment.[10] Compared to monodispersed cells, spheroid formation can further potentiate cell survival[11] and secretion of endogenous growth factors[12], motivating continued investigation into the mechanism and therapeutic effects of cell-cell communication within a

spheroid. This complex network of communication is orchestrated *via* signals from the microenvironment such as paracrine or autocrine-acting soluble factors[13] and intercellular communication through gap junctions, extracellular vesicles[14], and tunneling nanotubes (TNTs)[15]. TNTs are thin protrusions formed of actin microfilaments that transfer cytoplasm and organelles between connected cells.[16] TNTs have been reported in three-dimensional aggregates of cancerous cells[17] and more recently in MSC spheroids by our group.[18] These intercellular bridges shuttle cytoplasmic content and support distressed cells.[19,20] MSCs possess protective and restorative potential in co-culture systems that may be partially mediated by TNT formation between cells,[16] providing an opportunity to overcome the limitations of acquired senescence.

Spheroids offer a physiologically-relevant strategy to interrogate the dynamic nature of senescence resulting from intercellular communication. We hypothesized that intercellular communication mediated by TNTs would influence the expression of senescence markers in spheroids containing low and high passage MSCs. We formed spheroids using low passage, high passage, or a mixture of low and high passage MSCs and measured changes in senescence markers as a function of TNT formation. We verified the presence of TNTs using microscopy and flow cytometry. The functionality of TNTs was demonstrated by tracking and quantifying the exchange of cytoplasm and *p16* gene expression, a marker of cell senescence. These data represent the first demonstration of TNT-mediated augmentation of *p16* expression in spheroids and establish the importance of TNTs in spheroids.

MATERIALS AND METHODS

Cell culture

Human bone marrow-derived MSCs (Texas A&M Institute for Regenerative Medicine, Temple, TX) were received at passage 2 and pre-sorted to be: CD11b, CD19, CD34, CD45, CD79a, and CD117 negative equivalent to ≤ 2% and CD29, CD44, CD73a, CD90, and CD105 positive equivalent to ≥ 95%, and used without additional characterization. MSCs were expanded in standard culture conditions (37°C, 21% O_2, 5% CO_2) in α-MEM (Life Technologies, Carlsbad, CA) supplemented with 10% fetal bovine serum (FBS, Atlanta Biologicals, Flowery Branch, GA) and 1% penicillin/streptomycin (P/S, Gemini, Sacramento, CA) until use at passage 5 (P5, low passage) or 11 (P11, high passage).

To confirm the expression of senescence markers in higher passage cells, MSCs were plated at 30,000 cells/cm^2 and allowed to adhere overnight on tissue culture plastic. MSCs were stained using the senescence-activated β-galactosidase (SAβ-gal) staining kit per the manufacturer's instructions (Cell Signaling Technologies, Danvers, MA).

Spheroid formation and characterization

Spheroids were formed using a forced aggregation method.[21] Briefly, MSCs at P5 and/or P11 (4.35×10^5 cells/mL) were pipetted onto agarose molds in well plates, and the well plates were centrifuged at 500x*g* for 8 min. Plates were maintained statically in standard culture conditions for 48 h to form spheroids, each microwell containing 15,000 MSCs. To block TNT formation, cytochalasin D (CytoD, 500 nM, Sigma-Aldrich, St. Louis, MO) was added

to each well immediately after centrifugation, and cells were exposed for the full 48 h incubation.[18]

The diameter of live spheroids was measured using brightfield microscopy (Nikon Eclipse TE2000U microscope, Melville, NY). Spheroid diameter was calculated using NIS Elements (Nikon) by averaging the major and minor axis. Cell viability was assessed by a live/dead assay (Life Technologies). To measure cellular metabolic activity, spheroids were transferred to 24-well plates and incubated in 500 μL of α-MEM containing alamarBlue (Thermo Fisher, Waltham, MA) (10% v/v) for 30 min. MSC spheroids were collected in passive lysis buffer (Promega, Madison, WI), and DNA content was determined using the Quant-iT PicoGreen DNA Assay Kit (Invitrogen, Carlsbad, CA).

Scanning Electron Microscopy imaging

Sample preparation for scanning electron microscopy (SEM) characterization followed known protocols.[22] Briefly, spheroids underwent overnight fixation in 10% formalin (Thermo Fisher), and were resuspended in phosphate buffered saline (PBS, Mediatech, Herndon, VA). This suspension was pipetted onto poly-L-lysine-coated silicon wafers, followed by a multi-step dehydration process before being placed inside the SEM chamber. [18] Spheroids were imaged using a field emission SEM (S-4100T FE-SEM, Hitachi High Technologies America, Pleasanton, CA) under an accelerating voltage of 2 kV at 10 μA.

Quantification of cytosolic colocalization using laser scanning confocal microscopy

Prior to spheroid formation, MSCs were stained with 5 μM of CellTrace™ Far Red and/or Violet (Thermo Fisher) following the manufacturer's recommendations.[18] Spheroids were formed from cells with half the population dyed Red and the other half dyed Violet and termed 50:50 spheroids. In mixed passage spheroids, P5 MSCs were dyed Red and P11 MSCs were dyed Violet. MSCs dyed with both Red and Violet simultaneously prior to spheroid formation were termed dually-dyed spheroids.

Spheroids were imaged using laser scanning confocal microscopy (LSCM) (Fluoview 1000, Olympus America, Central Valley, PA). For Red-stained MSCs, LSCM images were collected between 640 and 740 nm under the excitation of 543 nm; while Violet-stained cells were imaged at 440 to 480 nm after excitation at 405 nm. All LSCM images were acquired simultaneously under the same detection conditions. The relative fluorescence intensity was quantified using ImageJ software. 25 single slices at depths from 5 to 29 μm, with 1 μm interlayer spacing, were obtained from 3 different spheroids in each group. The baseline relative fluorescence intensity of the colocalization of Red and Violet dyes was extracted from dually-dyed spheroids to establish the relative fluorescent intensity of the merged region. 50:50 spheroids were assessed for the amount of dye colocalization. Merged regions of each slice were calculated and divided by the total fluorescence area of the slice. The values from all slices were averaged in each group to represent the percentage of cytosol exchange.

Flow cytometry

Single cells within spheroids were analyzed by flow cytometry.[23] Briefly, spheroids were washed with PBS and dissociated in a solution of 0.1% (w/v) type I collagenase (Calbiochem, San Diego, CA) and 0.3 U dispase (Thermo Fisher) at 37°C with gentle external agitation. After 1 h, an equal volume of media was added to quench enzymatic activity, and cells were washed with PBS. Cells were resuspended in PBS, and fluorescence was analyzed by flow cytometry (AttuneNxt Flow Cytometer, Thermo Fisher). Flow cytometric analysis was performed using FlowJo (Version 10.5, FlowJo, LLC, Ashland, OR). Each treatment group was gated to remove ECM and background fluorescence from analysis. Single-stained, unstained, and dually-dyed samples were used to establish thresholds for each treatment group, and data are reported with background fluorescence subtracted from the compensated values. Each treatment group contained a minimum of 10,000 events.

Cell sorting (Astrios EQ, Beckman Coulter, Brea, CA) was performed on monodispersed cells after dissociation from spheroids. The cell counts for Red, Violet, and merged samples were quantified by the Astrios EQ software, and each group was collected for subsequent gene expression analysis.

Quantification of gene expression and protein secretion

Total RNA was collected using the Trizol RNA isolation protocol (Thermo Fisher), and 600 ng of total RNA was reverse-transcribed with the QuantiTect Reverse Transcription Kit (Qiagen, Valencia, CA). qPCR was performed using TaqMan1 Universal PCR Master Mix (Thermo Fisher). Primers and probes consisted of *p16* (Hs00923894_m1) and *RPL13* (Hs00204173_m1) (Thermo Fisher Scientific Life Sciences). qPCR results were normalized to the housekeeping transcript level (*RPL13*) and the control value of either P5 untreated or P5 CytoD-treated to yield $2^{-\Delta\Delta Ct}$,[24] or the housekeeping transcript level to yield $2^{-\Delta Ct}$.

Cytokine secretion was analyzed by quantifying the concentration of vascular endothelial growth factor (VEGF) and interleukin-6 (IL-6) in MSC spheroid conditioned media 24 h after spheroid formation using human-specific enzyme-linked immunosorbent assay (ELISA) kits (R&D Systems, Minneapolis, MN).

Statistical analysis

Data are presented as means ± standard deviation from at least three independent experiments. Statistical analysis was performed using a one-way analysis of variance with a Tukey's multiple comparison *post hoc* test or an unpaired Welch's t-test when applicable. All statistical analyses were performed using Prism 8 software (GraphPad, San Diego, CA); p values less than 0.05 were considered statistically significant. Significance is denoted by alphabetical letterings. Groups with no significance are linked by the same letters, whereas groups with significance do not share the same letters; ns denotes no significance among all groups.

RESULTS

Cells were cultured in monolayer until achieving designated passage numbers and stained for SAβ-gal. Unlike P5 MSCs, P11 MSCs exhibited positive SAβ-gal staining (Fig. 1A), establishing the presence of a common marker for senescence in high passage MSCs. Spheroids were formed from P5 MSCs, P11 MSCs, and a 50:50 combination of P5+P11 MSCs. Spheroids formed from P11 cells were significantly smaller than spheroids formed from P5 cells (Fig. 1B). However, no significant differences were detected in DNA content or metabolic activity between spheroids formed from high and/or low passage cells (Fig. 1C). In addition, high viability of the aggregated MSCs was maintained throughout all spheroids regardless of passage number (Fig. 1D).

We investigated the secretion of cytokines such as VEGF and IL-6 from MSC spheroids, as senescence in monolayer culture is often characterized by measuring the SASP.[25] However, the secretome of MSC spheroids differs significantly from cells in monolayer[26,27], limiting our ability to use changes in the secretome to definitively describe senescence. We observed decreases in VEGF (Fig. 2A) and IL-6 (Fig. 2B) secretion from spheroids as a function of MSC passage number. Protein secretion was partially (*i.e.*, VEGF) or near fully (*i.e.*, IL-6) restored when P5 MSCs were aggregated with P11 MSCs in P5+P11 spheroids.

SEM was used to detect the physical existence of TNT-like structures in P5, P11 and mixed P5+P11 spheroids to investigate if TNTs are involved in the modulation of senescence. TNT-like structures were detected in all MSC spheroid groups (Fig. 3). The observed intercellular connections were approximately 5–10 μm below the surface of the spheroid, exhibiting lengths between 1050–4900 nm and diameters varying from 30–190 nm, and thus consistent with other reports identifying TNTs.[18],[28]

TNTs are actin-rich structures that can be inhibited in the presence of CytoD.[18] To ensure that CytoD treatment did not impair MSC spheroid health, we evaluated the viability, total DNA content, and metabolic activity of spheroids within each group. Spheroids possessed high viability in all groups (Supplementary Fig. 1A), while no significant differences were detected in DNA content (Supplementary Fig. 1C) nor metabolic activity (Supplementary Fig. 1D) between spheroids formed from high or low passage cells or CytoD treatment. Notably, the diameter of MSC spheroids was changed as a function of passage number and actin polymerization inhibition (Supplementary Fig. 1B). The average spheroid diameter increased with CytoD treatment compared to the untreated counterpart in all groups. VEGF (Supplementary Fig. 1E) and IL-6 (Supplementary Fig. 1F) secretion from spheroids was changed as a function of MSC passage number, yet secretion of these factors was unaffected by addition of CytoD.

We explored whether TNTs observed between cells in spheroids of high and low passage cells were functional and could serve as a conduit to exchange cytosol between cells. We used confocal microscopy to image spheroids composed of MSCs stained in a 1:1 ratio with red or violet cytoplasmic dye (Fig. 4A). We observed distinct cell staining within both the red and violet channels. Upon overlaying the images from the red and violet channels, the

merged region of the image revealed areas where the dyes had colocalized, demonstrating transfer of cytosolic material (Fig. 4C). Untreated P5 MSC spheroids exhibited 20.0 ± 6.3% dye colocalization per total spheroid area (Fig. 4B). When treated with CytoD, the merged area of cytosolic dye decreased to 5.7 ± 2.9% (p=0.058). Dye colocalization was markedly reduced in spheroids formed from P11 MSCs, with only 8.7 ± 6.5% dye colocalization per total spheroid area, and this was further reduced to 1.0 ± 0.6% (p=0.523) when treated with CytoD. For spheroids composed of P5+P11 MSCs, the area of merged cytosolic dye was 16.3 ± 8.9% in untreated spheroids, statistically similar to untreated P5 spheroids (p=0.953), while CytoD-treated P5+P11 spheroids exhibited a reduction to 2.5 ± 1.6% (p=0.072).

To support our LSCM data and assess cytosol transfer throughout the entire spheroid, we quantified the extent of cytosolic exchange within each cell population using flow cytometry (Fig. 5A). Upon quantification of the merged regions, we observed that untreated P5 cells had the greatest degree of dye colocalization, 16.5 ± 1.9% of total cells (Fig. 5B). Cytosolic transfer was reduced to 4.9 ± 0.7% (p<0.0001) upon CytoD treatment. High passage cells had a similar rate of cytosolic transfer between untreated and CytoD-treated MSCs, 12.0 ± 0.8% and 10.9 ± 1.1% (p=0.971), respectively. This similarity is due to compromised cell membrane integrity of high passage MSCs and inability to distinctly retain the cytosolic dye after the digestion process (*data not shown*). When heterotypic spheroids were formed from P5 and P11 MSCs, dye colocalization was evident in 9.5 ± 2.0% of total cells in untreated spheroids, which decreased to 3.5 ± 1.4% (p=0.002) with CytoD treatment. The uniform distribution of dyed cells between each replicate is demonstrated by assessing the gated quadrants after the final cell count within each group (Fig. 5C).

We examined gene expression of *p16*, a regulatory protein marker of senescence[29], in whole spheroids containing low and high passage MSCs (Fig. 6A). MSC spheroids formed from P11 MSCs expressed high levels of *p16*, consistent with other indicators of senescence such as morphology and SAβ-gal staining in monolayer culture. When P5 MSCs were included in the spheroid, overall *p16* expression decreased by more than 90% (p<0.0001), suggesting a rescue-like decrease in senescence (Fig. 6B). When exposed to CytoD, the effect of P5 cells was less pronounced but still reduced global *p16* expression by 18% (p=0.046) (Fig. 6C). In order to evaluate *p16* expression in each cell population rather than as a whole aggregate, we dissociated cells from spheroids into low and high passage MSCs (Fig. 6D). In agreement with flow cytometry, CytoD treatment decreased cytosol transfer between low and high passage MSCs in P5+P11 spheroids from 11.5 ± 1.0% to 3.9 ± 0.3% (p=0.007) (Fig. 6E). The subsequent gene expression of *p16* in isolated low and high passage MSCs showed an equivalent degree of senescence when previously aggregated in untreated spheroids. However, we detected a significant increase in *p16* expression in P11 MSCs within CytoD-treated spheroids (Fig. 6F), confirming that P11 MSCs benefit from the colocalization of P5 MSCs and TNT transfer of cellular constituents that reduce markers of senescence.

Using the forward scatter from our flow sort data, we determined that high passage MSCs have a smaller median area compared to low passage MSCs when in suspension (Supplementary Table 1). In addition, the median area of untreated MSCs was smaller than the corresponding CytoD-treated group. These data correlate to a smaller measured average

diameter of P11 spheroids and an increase in the average spheroid diameter with CytoD treatment compared to untreated cells in all groups (Supplementary Fig. 1B).

DISCUSSION

MSCs represent approximately 0.01% of mononucleated cells in bone marrow aspirate[30], a common tissue compartment for MSC collection, requiring increased aspirate volume and/or prolonged culture expansion to achieve the necessary quantity of cells. MSCs lose their potency at higher passages due to replicative senescence, necessitating the use of MSCs at low passage numbers[31] and presenting a challenge to achieve clinically relevant numbers for cell-based therapies. Since cell senescence is a dynamic process[5] and the senescent phenotype is not damaging to the overall health of an organism[6], strategies that reverse or reduce senescence provide a much-needed opportunity to utilize higher passage cells. MSCs can protect or support distressed cells by transferring cellular material using TNTs.[19] In this study, we explored the ability of lower passage MSCs, when formed into spheroids, to suppress the expression of senescence markers in higher passage MSCs *via* TNTs as a first step to retain their therapeutic potential.

MSCs have the potential to contribute to tissue regeneration in many ways, including differentiation toward a desired phenotype, trophic factor secretion, and ECM production.[32] For example, the addition of MSCs decreased the dependence on low passage primary chondrocytes by maintaining a stable desired phenotype during culture.[33] In fact, MSC-chondrocyte co-culture improved the chondrogenic and proliferative potentials of engineered cartilage compared to chondrocytes alone.[34] This beneficial effect was observed between primary chondrocytes from elderly donors (mean age of 66.3 years) and MSCs from middle-aged donors (mean age of 59.2 years)[35], confirming that even older MSCs could be used as “instructor” cells. To date, most studies characterize senescence in monolayer culture, which lacks physiological relevance to tissues *in vivo*. Others have demonstrated the TNT-dependent reduction of senescent markers in endothelial cells.[36] Nonetheless, for the first time, we demonstrate the capacity of low passage MSCs to abrogate the acquired senescence phenotype of high passage MSCs during direct cell-cell contact in three-dimensional spheroids.

MSCs use multiple mechanisms to communicate and influence surrounding cells such as endogenously produced signaling factors, extracellular vesicles[37], direct cell-cell contact with gap junctions, and TNTs.[15] In these studies, we examined the contribution of TNTs toward intercellular communication and their effect on senescence. Though the regulatory pathways affected by actin polymerization for TNT formation and exosomes are overlapping, our data support that the colocalization of dyed cytosol is due to functional TNTs. We observed TNT-like structures using SEM and confocal microscopy and a reduction of cytosol colocalization in higher passage MSCs. Moreover, extracellular vesicle release increases with cellular senescence[38,39], yet the degree of cytosolic exchange in these studies decreased with higher passage MSCs. Gap junctions exchange ions and small metabolites between adjacent cells, but relatively little cytoplasm is transferred in the process. Further studies are needed to determine potential synergies between intercellular

communication mechanisms such as direct cell-cell and cell-matrix contact or secretion of soluble factors on MSCs.

We investigated the role of intercellular communication on the dynamic nature of senescence within MSC spheroids. The arrest of the cell-cycle within MSCs has been documented using several indices, including an inability to differentiate, the SASP, and enhanced gene expression of regulatory proteins.[25] We measured VEGF and IL-6 secretion since these cytokines are associated with the SASP and are implicated in paracrine signaling when using MSCs in cell-based tissue engineering. Notably, VEGF and IL-6 secretion were reduced in spheroids formed from high passage MSCs compared to low passage cells, and this effect was partially restored when P11 MSCs were combined with P5 MSCs in spheroid form. However, we could not rely solely on the SASP because senescence has been characterized by changes in cytokine secretion in monolayer culture[40], including increased VEGF[41] and IL-6[42,43] production by senescent cells. Since spheroid formation markedly influences the MSC secretome compared to monolayer or monodispersed cells[12,23], cytokine secretion was insufficient to assess senescence in MSC spheroids.

p16 is a cyclin-dependent kinase inhibitor acting upstream of retinoblastoma (RB) tumor suppressor, a master regulator of the cell cycle.[44] The RB pathway is essential for induction of senescence in human cells.[45] P11 spheroids exhibited high *p16* expression, corroborating senescence in high passage cells. Moreover, *p16* expression was downregulated when P11 MSCs were combined with P5 MSCs within the same spheroid. While still evident, we observed a marked reduction in *p16* expression in P5+P11 spheroids that underwent CytoD treatment to abrogate TNTs. Others have shown that targeted overexpression of certain genes in MSCs can inhibit oxidative stress and inactivate the *p16* signaling pathway.[46] Such work supports our claim that MSCs can affect the expression of *p16* in other MSCs. Upon sorting mixed passage MSCs from spheroids, we observed increased expression of *p16* in P11 MSCs compared to P5 cells from the same spheroid. Furthermore, the magnitude of *p16* expression was significantly higher in P11 MSCs when the aggregate was formed in the presence of CytoD. To the best of our knowledge, these studies are the first to demonstrate a restorative effect from MSC to MSC through TNT formation. Further studies are needed to determine the identity of the cytoplasmic payload transferred between cells.

LSCM is a valuable tool to visualize the transfer of cytosol among cells in spheroids. In these studies, LSCM was focused on the periphery of the spheroid due to limitations in light penetration. We used flow cytometry to characterize cytosol transfer between cells throughout the entire spheroid, and these data were in agreement with LSCM results. We observed similar levels of dyed cells within a spheroid regardless of passage number or treatment group, thereby confirming the 50:50 mixture of low and high passage cells within a mixed passage spheroid. Reductions in cell membrane integrity represent another characteristic of senescent cells[47], and dissociation of the spheroids into monodispersed cells for flow cytometry compromised the cell membranes in P11 MSCs. However, this compromised integrity was not observed when P11 MSCs were cultured with P5 MSCs. Thus, dye transfer between low and high passage MSCs in spheroids allowed us to study the role of TNTs in mediating senescence markers within heterotypic spheroids. We used CytoD

to inhibit actin polymerization and tubule formation in low and high passage MSCs. Similar approaches have been used to restore elasticity in aged human epithelial cells.[48] The use of CytoD on senescent MSCs appears to inhibit the functionality of TNTs within MSC spheroids. The quantification and effect of cytosolic transfer by TNTs in mixed passage spheroids was corroborated by changes in *p16* gene expression. Lastly, we acknowledge that MSCs are a heterogeneous population of cells and that senescence within these cells is also heterogeneous. Further studies are needed to evaluate cell-cell communication in a more homogeneous cell population at early and late passages.

CONCLUSION

These studies establish that TNTs form among MSCs in three-dimensional culture regardless of cell passage number. The level of cytosolic transfer *via* functional TNTs is decreased with CytoD treatment, especially for spheroids containing low passage cells. Moreover, senescence-associated gene expression of the regulatory protein *p16* can be diminished through the addition of low passage MSCs to the spheroid. This mutable level of a senescence-associated marker is at least partially mediated by TNTs. These data demonstrate the promise of spheroids composed of low and high passage cells to decrease senescence of MSCs during *in vitro* culture, providing an opportunity to maintain the regenerative properties of culture-expanded MSCs for cell-based tissue engineering therapies.

Supplementary Material

Refer to Web version on PubMed Central for supplementary material.

ACKNOWLEDGEMENTS

This work was supported by the National Institutes of Health under award number R01 DE025475 (JKL), R21 ES025350 (GYL) and the Gordon and Betty Moore Foundation (GYL). JW was supported by a National Science Foundation Graduate Research Fellowship (1650042) and the Achievement Rewards for College Scientists (ARCS) Foundation fellowship. JNH received support from the National Defense Science and Engineering Graduate Fellowship (32 CFR 168a), Schwall Fellowship in Medical Research, and the ARCS Foundation fellowship. The content is solely the responsibility of the authors and does not necessarily represent the official views of the funding agencies.

REFERENCES

1. Leach JK, Whitehead J. Materials-Directed Differentiation of Mesenchymal Stem Cells for Tissue Engineering and Regeneration. ACS Biomater Sci Eng 2018;4:1115–1127. [PubMed: 30035212]
2. Murphy MB, Moncivais K, Caplan AI. Mesenchymal stem cells: environmentally responsive therapeutics for regenerative medicine. Exp Mol Med 2013;45:e54. [PubMed: 24232253]
3. Banfi A, Muraglia A, Dozin B, et al. Proliferation kinetics and differentiation potential of ex vivo expanded human bone marrow stromal cells: Implications for their use in cell therapy. Exp Hematol 2000;28:707–715. [PubMed: 10880757]
4. Muñoz-Espín D, Serrano M. Cellular senescence: from physiology to pathology. Nat Rev Mol Cell Biol 2014;15:482–496. [PubMed: 24954210]
5. Schmitt CA. The persistent dynamic secrets of senescence. Nat Cell Biol 2016;18:913–915. [PubMed: 27571737]
6. Young ARJ, Narita M, Narita M. Cell Senescence as Both a Dynamic and a Static Phenotype BT Totowa, NJ: Humana Press, 2013.

7. Storer M, Mas A, Robert-Moreno A, et al. Senescence Is a Developmental Mechanism that Contributes to Embryonic Growth and Patterning. Cell 2013;155:1119–1130. [PubMed: 24238961]
8. Jun J-I, Lau LF. The matricellular protein CCN1 induces fibroblast senescence and restricts fibrosis in cutaneous wound healing. Nat Cell Biol 2010;12:676–685. [PubMed: 20526329]
9. Krizhanovsky V, Yon M, Dickins RA, et al. Senescence of activated stellate cells limits liver fibrosis. Cell 2008;134:657–667. [PubMed: 18724938]
10. Murphy KC, Hung BP, Browne-Bourne S, et al. Measurement of oxygen tension within mesenchymal stem cell spheroids. J R Soc Interface 2017;14:20160851. [PubMed: 28179546]
11. Ho SS, Murphy KC, Binder BYK, et al. Increased Survival and Function of Mesenchymal Stem Cell Spheroids Entrapped in Instructive Alginate Hydrogels. Stem Cells Transl Med 2016;5:773–781. [PubMed: 27057004]
12. Murphy KC, Fang SY, Leach JK. Human mesenchymal stem cell spheroids in fibrin hydrogels exhibit improved cell survival and potential for bone healing. Cell Tissue Res 2014;357:91–99. [PubMed: 24781147]
13. Blüthgen N, Legewie S. Robustness of signal transduction pathways. Cell Mol Life Sci 2013;70:2259–2269. [PubMed: 23007845]
14. Liu S, Mahairaki V, Bai H, et al. Highly Purified Human Extracellular Vesicles Produced by Stem Cells Alleviate Aging Cellular Phenotypes of Senescent Human Cells. Stem Cells 2019.
15. Ariazi J, Benowitz A, De Biasi V, et al. Tunneling Nanotubes and Gap Junctions-Their Role in Long-Range Intercellular Communication during Development, Health, and Disease Conditions. Front Mol Neurosci 2017;10:e333.
16. Marzo L, Gousset K, Zurzolo C. Multifaceted roles of tunneling nanotubes in intercellular communication. Front Physiol 2012;3:e72.
17. Patheja P, Dasgupta R, Dube A, et al. The use of optical trap and microbeam to investigate the mechanical and transport characteristics of tunneling nanotubes in tumor spheroids. J Biophotonics 2015;8:694–704. [PubMed: 25355694]
18. Zhang J, Whitehead J, Liu Y, et al. Direct Observation of Tunneling Nanotubes within Human Mesenchymal Stem Cell Spheroids. J Phys Chem B 2018;122:9920–9926. [PubMed: 30350968]
19. Vignais M-L, Caicedo A, Brondello J-M, et al. Cell connections by tunneling nanotubes: Effects of mitochondrial trafficking on target cell metabolism, homeostasis, and response to therapy. Stem Cells Int 2017:e6917941.
20. Jackson M V, Krasnodembskaya AD. Analysis of Mitochondrial Transfer in Direct Co-cultures of Human Monocyte-derived Macrophages (MDM) and Mesenchymal Stem Cells (MSC). Bio-Protocol 2017;7:e2255. [PubMed: 28534038]
21. Vorwald CE, Ho SS, Whitehead J, et al. High-Throughput Formation of Mesenchymal Stem Cell Spheroids and Entrapment in Alginate Hydrogels - Biomaterials for Tissue Engineering: Methods and Protocols. In: Chawla K, ed. Biomater. Tissue Eng, New York, NY: Springer New York, 2018:139–149.
22. Liu Y, Wang K-H, Chen H-Y, et al. Periodic Arrangement of Lipopolysaccharides Nanostructures Accelerates and Enhances the Maturation Processes of Dendritic Cells. ACS Appl Nano Mater 2018;1:839–850.
23. Grässer U, Bubel M, Sossong D, et al. Dissociation of mono- and co-culture spheroids into single cells for subsequent flow cytometric analysis. Ann Anat - Anat Anzeiger 2018;216:1–8.
24. Schmittgen TD, Livak KJ. Analyzing real-time PCR data by the comparative CT method. Nat Protoc 2008;3:1101–1108. [PubMed: 18546601]
25. Coppé J-P, Desprez P-Y, Krtolica A, et al. The Senescence-Associated Secretory Phenotype: The Dark Side of Tumor Suppression. Annu Rev Pathol 2010;5:99–118. [PubMed: 20078217]
26. Redondo-Castro E, Cunningham CJ, Miller J, et al. Changes in the secretome of tri-dimensional spheroid-cultured human mesenchymal stem cells in vitro by interleukin-1 priming. Stem Cell Res Ther 2018;9:1–11. [PubMed: 29291747]
27. Murphy KC, Whitehead J, Falahee PC, et al. Multifactorial Experimental Design to Optimize the AntiInflammatory and Proangiogenic Potential of Mesenchymal Stem Cell Spheroids. Stem Cells 2017;35:1493–1504. [PubMed: 28276602]

28. Yang H, Borg TK, Ma Z, et al. Biochip-based study of unidirectional mitochondrial transfer from stem cells to myocytes via tunneling nanotubes. Biofabrication 2016;8:15012.
29. Liu J-Y, Souroullas GP, Diekman BO, et al. Cells exhibiting strong p16INK4a promoter activation in vivo display features of senescence. Proc Natl Acad Sci 2019;116:2603–2611. [PubMed: 30683717]
30. Alvarez-Viejo M, Menendez-Menendez Y, Blanco-Gelaz MA, et al. Quantifying Mesenchymal Stem Cells in the Mononuclear Cell Fraction of Bone Marrow Samples Obtained for Cell Therapy. Transplant Proc 2013;45:434–439. [PubMed: 23375334]
31. Tan AR, Alegre-Aguarón E, O'Connell GD, et al. Passage-dependent relationship between mesenchymal stem cell mobilization and chondrogenic potential. Osteoarthr Cartil 2015;23:319–327. [PubMed: 25452155]
32. Galipeau J, Sensébé L. Mesenchymal Stromal Cells: Clinical Challenges and Therapeutic Opportunities. Cell Stem Cell 2018;22:824–833. [PubMed: 29859173]
33. Meretoja V V, Dahlin RL, Wright S, et al. The effect of hypoxia on the chondrogenic differentiation of co-cultured articular chondrocytes and mesenchymal stem cells in scaffolds. Biomaterials 2013;34:4266–4273. [PubMed: 23489925]
34. Kang N, Liu X, Guan Y, et al. Effects of co-culturing BMSCs and auricular chondrocytes on the elastic modulus and hypertrophy of tissue engineered cartilage. Biomaterials 2012;33:4535–4544. [PubMed: 22440049]
35. Giovannini S, Diaz-Romero J, Aigner T, et al. Micromass co-culture of human articular chondrocytes and human bone marrow mesenchymal stem cells to investigate stable neocartilage tissue formation in vitro. Eur Cells Mater 2010;20:245–259.
36. Yasuda K, Khandare A, Burianovskyy L, et al. Tunneling nanotubes mediate rescue of prematurely senescent endothelial cells by endothelial progenitors : exchange of lysosomal pool. Aging (Albany NY) 2011;3:597–608. [PubMed: 21705809]
37. van Niel G, D'Angelo G, Raposo G. Shedding light on the cell biology of extracellular vesicles. Nat Rev Mol Cell Biol 2018;19:213–228. [PubMed: 29339798]
38. Lehmann BD, Paine MS, Brooks AM, et al. Senescence-associated exosome release from human prostate cancer cells. Cancer Res 2008;68:7864–7871. [PubMed: 18829542]
39. Takahashi A, Okada R, Nagao K, et al. Exosomes maintain cellular homeostasis by excreting harmful DNA from cells. Nat Commun 2017;8:1–14. [PubMed: 28232747]
40. Rodier F, Coppé J-P, Patil CK, et al. Persistent DNA damage signalling triggers senescence-associated inflammatory cytokine secretion. Nat Cell Biol 2009;11:973–979. [PubMed: 19597488]
41. Coppe JP, Kauser K, Campisi J, et al. Secretion of vascular endothelial growth factor by primary human fibroblasts at senescence. J Biol Chem 2006;281:29568–29574. [PubMed: 16880208]
42. O'Hagan-Wong K, Nadeau S, Carrier-Leclerc A, et al. Increased IL-6 secretion by aged human mesenchymal stromal cells disrupts hematopoietic stem and progenitor cells' homeostasis. Oncotarget 2016;7:13285–13296. [PubMed: 26934440]
43. Di G-H, Liu Y, Lu Y, et al. IL-6 secreted from senescent mesenchymal stem cells promotes proliferation and migration of breast cancer cells. PLoS One 2014;9:e113572. [PubMed: 25419563]
44. Kuilman T, Michaloglou C, Mooi WJ, et al. The essence of senescence. Genes Dev 2010;24:2463–2479. [PubMed: 21078816]
45. Giacinti C, Giordano A. RB and cell cycle progression. Oncogene 2006;25:5220–5227. [PubMed: 16936740]
46. Chen G, Zhang Y, Yu S, et al. Bmi1 Overexpression in Mesenchymal Stem Cells Exerts Anti-Aging and Anti-Osteoporosis Effects by Inactivating p16/p19 Signaling And Inhibiting Oxidative Stress. Stem Cells 2019.
47. DiLoreto R, Murphy CT. The cell biology of aging. Mol Biol Cell 2015;26:4524–4531. [PubMed: 26668170]
48. Sokolov I, Iyer S, Woodworth CD. Recovery of elasticity of aged human epithelial cells In Vitro. Nanomedicine 2006;2:31–36. [PubMed: 17292113]

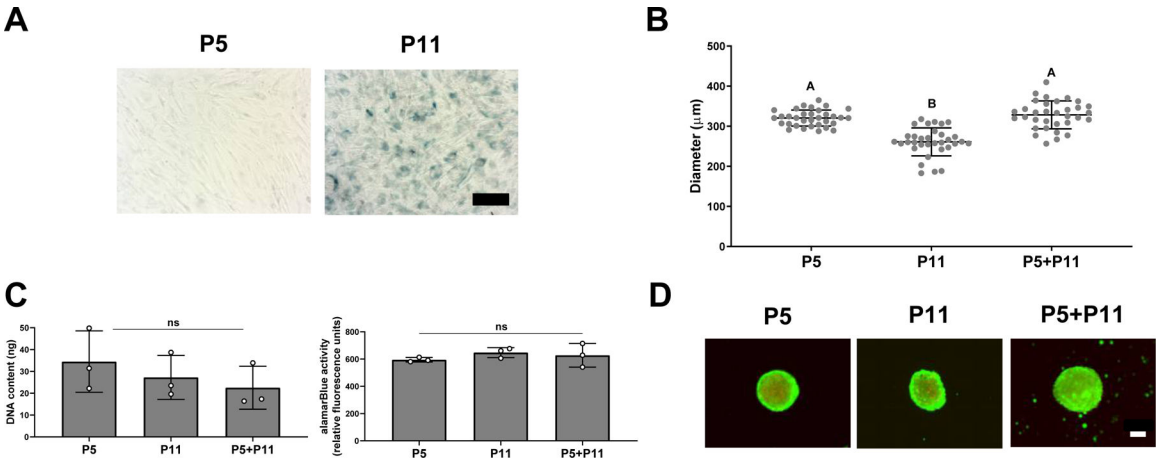

Figure 1. MSC spheroid diameter is influenced by passage number.

(A) SAβ-gal senescent staining of P5 and P11 MSCs; blue indicates positive staining. Scale bar is 100 μm. **(B)** Quantification of spheroid diameter using MSCs at P5, P11, and P5+P11 (n=33 per group). **(C)** Left: DNA content of P5, P11, and P5+P11 MSC spheroids (n=3). Right: Metabolic activity of P5, P11, and P5+P11 MSC spheroids (n=3). **(D)** Representative live/dead images of P5, P11, and P5+P11 MSC spheroids; live cells are green and dead cells are red. Scale bar is 100 μm.

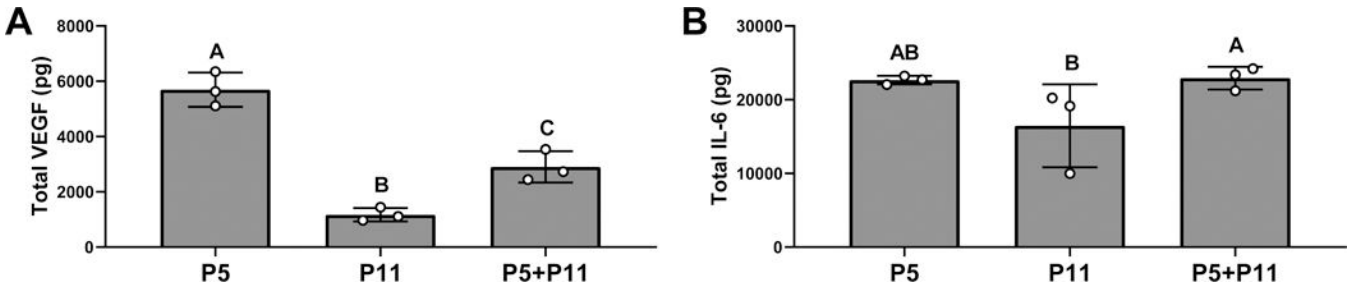

Figure 2. Cytokine secretion from MSC spheroids is influenced by passage number.

Total **(A)** VEGF and **(B)** IL-6 secretion by MSC spheroids as a function of passage number (n = 3 per group).

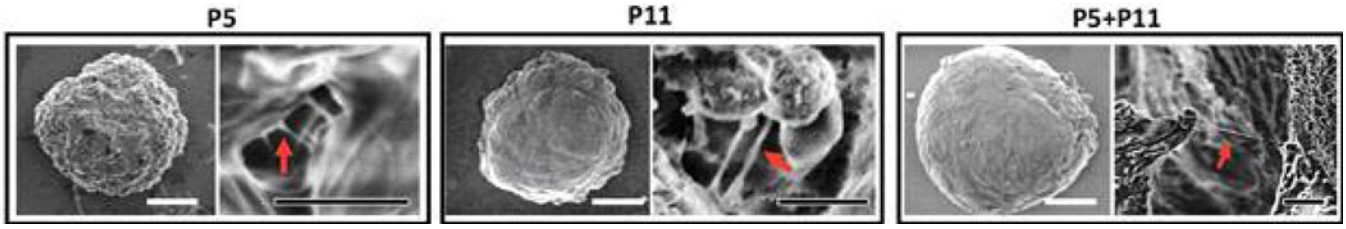

Figure 3. TNT-like protrusions are observed in MSC spheroids regardless of passage number.
Representative SEM images confirm TNT-like structures between two cells (indicated by red arrows) within P5, P11, and P5+P11 MSC spheroids. Scale bars are 60 μm and 1 μm for white and black bars, respectively.

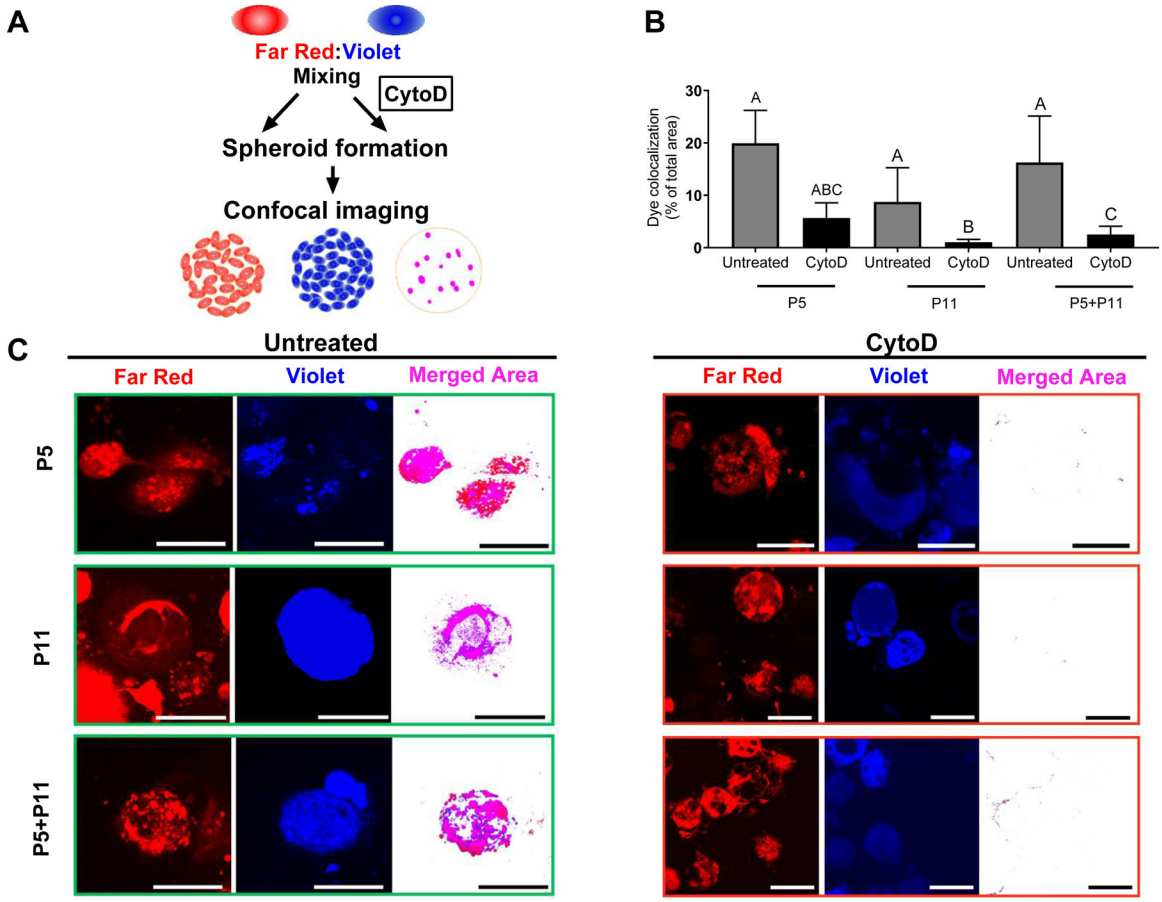

Figure 4. Transfer of cytosolic dyes is detectable by fluorescence.

(A) Schematic of experimental method for staining MSCs and identifying regions of fluorescence for quantification. **(B)** Quantification of the percent area representing merged fluorescence as an indicator of cytosolic dye transfer (n=3 for all groups). **(C)** Representative LSCM single-sliced images demonstrate the fluorescent area in the red and violet channels, with the overlaid area revealing colocalization of the red and violet dyes. Scale bars are 20 μm.

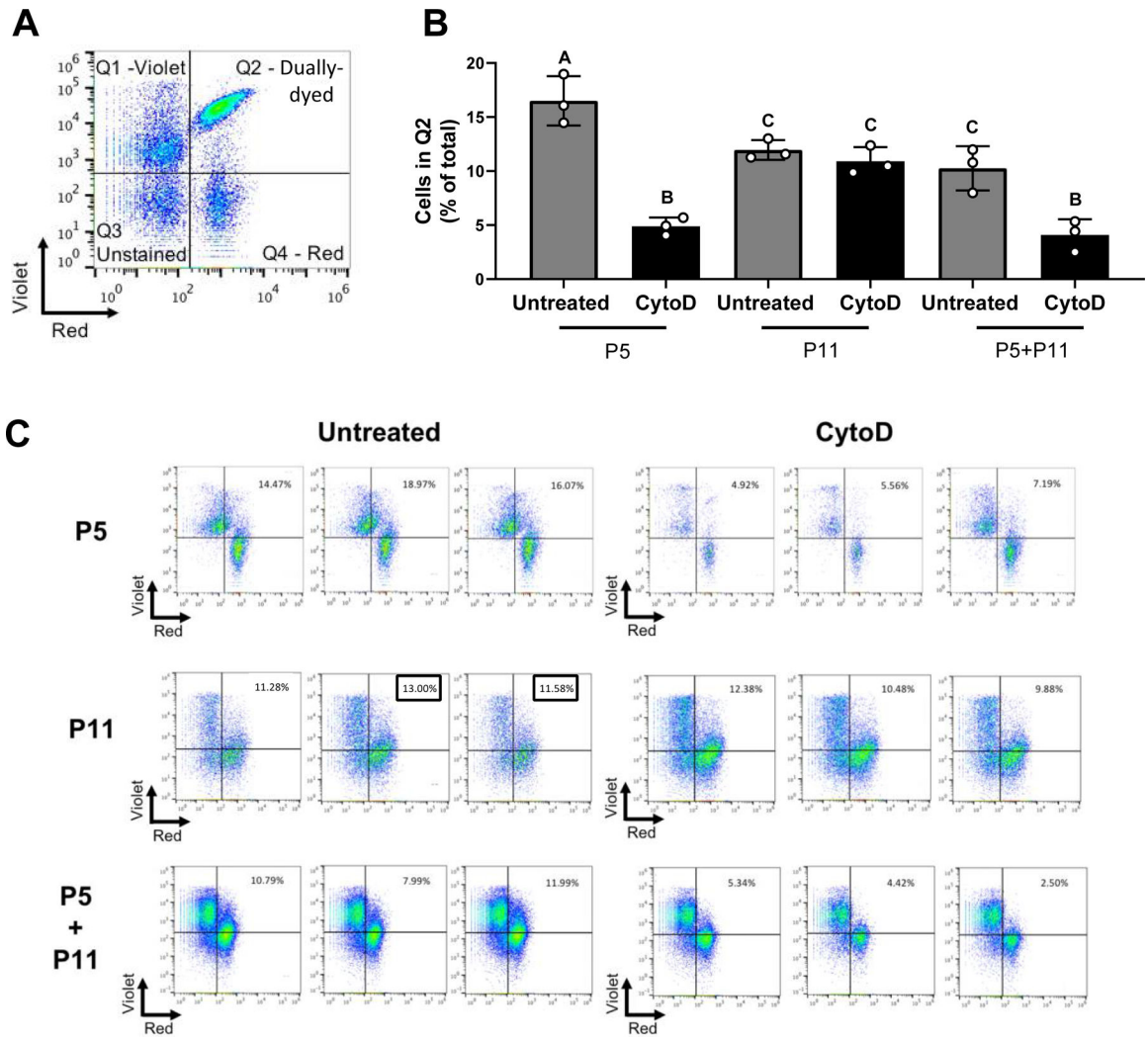

Figure 5. The frequency of cytosolic dye colocalization was quantified by flow cytometry.

(A) Representative image of the control groups used to establish gating; quadrants are labeled with corresponding dyes to identify cells. **(B)** Quantification of merged red and violet dye located in quadrant 2 (n=3 per group). **(C)** Representative images of all four quadrants from each replicate of flow cytometry to visually demonstrate the distribution of dyed cells.

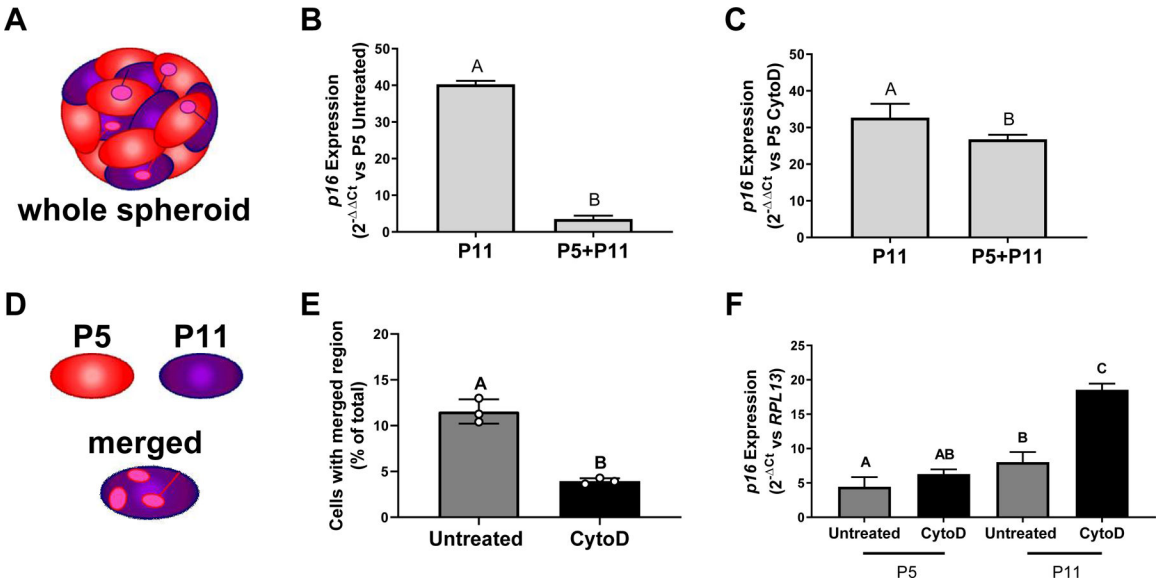

Figure 6. Low passage MSCs abrogate *p16* expression in high passage cells in MSC spheroids.

(A) Schematic denoting that data in this row represent quantification of gene expression from whole spheroids. **(B)** Quantification of *p16* expression in P11 and P5+P11 untreated MSC spheroids (n=4 per group). **(C)** Quantification of *p16* expression in P11 and P5+P11 CytoD treated MSC spheroids (n=4 per group). **(D)** Schematic denoting that data in this row are a quantification of cell populations isolated from whole spheroids following cell sorting. **(E)** Quantification of MSCs dissociated from mixed P5+P11 spheroids containing merged red and violet dye (n=3 per group). **(F)** Quantification of *p16* expression of P5 and P11 MSCs in the absence or presence of CytoD treatment during spheroid formation (n=4 per group).